fishes

MDPI

Article

Rodlet Cells Provide First Line of Defense against Swimbladder Nematode and Intestinal Coccidian in *Anguilla anguilla*

Bahram Sayyaf Dezfuli [1,*], Giuseppe Castaldelli [2], Massimo Lorenzoni [3], Antonella Carosi [3], Mykola Ovcharenko [4] and Giampaolo Bosi [5]

[1] Department of Life Sciences and Biotechnology, University of Ferrara, St. Borsari 46, 44121 Ferrara, Italy
[2] Department of Environmental and Prevention Sciences, University of Ferrara, St. Borsari 46, 44121 Ferrara, Italy
[3] Department of Cellular and Environmental Biology, University of Perugia, St. Elce di Sotto 5, 06123 Perugia, Italy
[4] Institute of Biology and Environment Protection, Pomeranian University, Arciszewskiego 22, 76-218 Słupsk, Poland
[5] Department of Veterinary Medicine and Animal Science, University of Milan, St. of University 6, 26900 Lodi, Italy
* Correspondence: dzb@unife.it

Abstract: A subpopulation of 97 European eels, *Anguilla anguilla*, was obtained from a local consortium of Lake Trasimeno. The fish were examined for parasites in the swimbladder (SB) and intestine; the SBs of 66 (68%) of the 97 eels contained 480 adult specimens of the nematode *Anguillicoloides crassus* (Kuwahara, Niimi and Itagaki, 1974) and the intensity of infection ranged from 1 to 18 adult worms per SB (7.27 ± 0.43, mean ± SE). In heavily infected SB, the wall was thicker; upon excision, black-brownish adult nematodes were noticed inside the lumen. The infected SBs showed a papillose aspect of the epithelium and frequent erosion, inflammation, hemorrhages, and dilation of blood vessels. In parasitized SBs, mast cells and macrophages were encountered in the mucosal layer; in several heavily infected SB, rodlet cells were the sole fish immune cells noticed in the epithelium and in close contact with the *A. crassus*. With reference to the eel intestinal epithelium, in fifteen eels, two developmental stages of coccidian were close to clusters of rodlet cells, the coccidian induced erosion of the epithelium. The results of a panel of 12 antibodies in the European eel infected tissues will be presented.

Keywords: eel; swimbladder; nematode; intestine; coccidian; rodlet cells; immunohistochemistry

check for updates

Citation: Sayyaf Dezfuli, B.; Castaldelli, G.; Lorenzoni, M.; Carosi, A.; Ovcharenko, M.; Bosi, G. Rodlet Cells Provide First Line of Defense against Swimbladder Nematode and Intestinal Coccidian in *Anguilla anguilla*. *Fishes* **2023**, *8*, 66. https://doi.org/10.3390/fishes8020066

Academic Editor: María Ángeles Esteban

Received: 22 December 2022
Revised: 18 January 2023
Accepted: 19 January 2023
Published: 21 January 2023

Copyright: © 2023 by the authors. Licensee MDPI, Basel, Switzerland. This article is an open access article distributed under the terms and conditions of the Creative Commons Attribution (CC BY) license (https://creativecommons.org/licenses/by/4.0/).

1. Introduction

The European eel *Anguilla anguilla* (Linnaeus, 1758) reproduces in the Sargasso Sea after a spawning migration of more than 5000 km in about 5 months. Due to such a long journey, the eel swimbladder (SB) is under physiological stress. The SB is a hydrostatic organ responsible for neutral buoyancy [1]. *Anguillicoloides crassus* (Nematoda) is a well-known parasite of the SB in six species of eel [2].

The success of the eel's spawning migration depends on the health and proper function of the SB; several accounts report that the nematode *A. crassus* impairs SB function [1–3] and can compromise the reproductive migration of the host [1]. This parasite affects the cellular and humoral immune response of the eel SB [4] and the physiological status of the infected SB [5]. The European eel is considered a critically endangered species due to several factors [6], with *A. crassus* presumed to be one of the reasons for the dramatic decline of the *A. anguilla* numbers [1].

Helminths are metazoan worm parasites that have evolved a number of unique adaptations to regulate, manipulate or even evade the host immune system [7]. This masterful adaptation is due to their long coevolution with the hosts and enables the

helminths to effectively modulate the immune system [8]. In the intestinal tract and in the airways, barrier integrity can be physically compromised by helminth parasites [7,9]. In fish, the mucosal layer of most organs (e.g., skin, gills, digestive tract, SB, gonads) form a physical barrier providing the first line of defense against infection [3,9,10]. Whenever this mucosal barrier is damaged/disturbed at a point-region, resident immune cells are activated, and tissue-specific leukocytes are recruited from the blood to the infection site [10]. The role of the mucosal immune response of the skin of *A. anguilla* against *Vibrio anguillarum* was detailed recently in Conforto et al. [11].

The SB is an unpaired organ and, like intestine, liver, and pancreas, is endoderm-derived [12]. In the mucosal layer of infected SBs, numerous mast cells (MCs), macrophages (MAs) and rodlet cells (RCs) are encountered; more accounts of the occurrence of granulocytes and MAs in eel swimbladders infected with *A. crassus* are in Würtz and Taraschewski [13], Knopf [4], Sayyaf Dezfuli [3].

In 15 eels, the intestinal epithelium was infected with two developmental stages of a coccidian. Coccidians are intracellular protozoan parasites belonging to the phylum Apicomplexa [14]. The presence of coccidians in fish was mentioned in Kristmundsson et al. [15] and Matsche et al. [16], and in eel it was reported in Molnar and Baska [17], in Benajib et al. [18], and in Hine [19]. Herein, we focused our attention mainly on markers (12 antibodies) in the immune cells (e.g., MCs, MAs and RCs) of eel SB and intestine. An emphasis was placed on RCs because they were the sole cells in the SB epithelium that were very close to the nematode and in contact with the coccidian infecting the eel intestine. Finally, we present a brief account of the function and importance of most of the above antibodies found in host immune cells.

A large amount of histamine is stored in cytoplasmic granules of MCs and is quickly secreted in response to immunological stimuli [20]. The first account of the occurrence of histamine in fish intestinal MCs was provided by Mulero et al. [21]. Following that initial report, histamine was documented in fish enteric immune cells in the presence of parasites [22,23]. In the intestine of teleosts, serotonin serves as a pro-inflammatory molecule secreted and stored in different types of cells [22] and has several functions [9,24,25]. Numerous MCs containing serotonin were observed in the intestine of fish harboring helminths [23]. Herein, data on the immunoreactivity of MCs and presumable MAs in the infected SB and intestine of eels to two different anti-serotonin antibodies will be provided. In addition to histamine and serotonin, granules of MCs contain proteases such as tryptase and chymase [21,26].

Toll-like receptors (TLRs) are antimicrobial peptides of the innate and adaptive immune systems [27]; they belong to the Pattern Recognition Receptors (PRRs) [28]. In the European eel, various signal molecules were detected in intestinal RCs, among them inducible-nitric oxide synthase (i-NOS) [29]. DePasquale [30] reported an accumulation of tropomyosin at the apical tip of the RCs, forming a cap-like structure. Tropomyosin is a component of the contraction system in different cells and tissues [31,32]. The molecules of tropomyosin regulate the Ca^{2+}-dependent interaction of myosin heads with actin myofilaments [32].

Most of the mechanisms involved in the interaction between fish and their parasites are still unknown. The current investigation was undertaken to gain additional information on the presence and distribution of 12 antibodies expressed by MCs, MAs, and RCs.

2. Materials and Methods

A subpopulation of 97 *A. anguilla* with total length ranging from 35.0 to 58.2 cm (46.09 ± 0.56 cm, mean ± SE) and weighing from 71.5 to 339.6 g (157.34 ± 6.98 g, mean ± SE) were provided on several occasions from July 2019 to July 2021 in Lake Trasimeno (Central Italy, 43°9′11″ N and 12°15′ E) by professional fishermen of a local consortium using fyke nets. The eels were transferred alive to the Department of Cellular and Environmental Biology, University of Perugia. Immediately in the laboratory, the fish were euthanized with an overdose of MS222 (125 mg L^{-1}, tricaine methanesulfonate, Sandoz, Basel, Switzerland).

Afterward, the spinal cords were severed before the eels were dissected ventrally; then, the whole digestive tract was removed to allow the extraction of the SB from the fish's body.

Each SB and intestine were opened longitudinally to search for parasites; from a subpopulation of both organs (40 infected and 7 uninfected SB and 40 intestine), some 15 × 15 mm pieces were excised and fixed in 10% neutral buffered formalin for 24 h. Then, the samples were dehydrated through an alcohol series and paraffin wax-embedded using a Shandon Citadel 2000 tissue processor (London, UK). Multiple 5 µm sections were taken from each tissue block, stained with Haematoxylin and Eosin and/or Giemsa or Alcian Blue, and examined and photographed using a Nikon Microscope ECLIPSE 80i (Tokyo, Japan).

The immunohistochemical tests were carried out on 5 µm thick sections of uninfected and parasitized eel tissues using a panel of 12 antibodies against markers of immune cells (Table 1). In our lab, we have frequently and successfully employed these antibodies to reveal immune cells in the gut of numerous fish species [3,22,23,33]. After dewaxing and rehydration, the sections were treated for 20 min with 3% H_2O_2 in Tris-buffered saline (TBS) pH 7.6 (TBS: 0.05 M Tris-HCl, 0.15 M NaCl) to block endogenous peroxidase. Then, sections were rinsed 2 × 5 min in TBS and incubated for 30 min with 1:20 goat normal serum to block tissue-unspecific binding sites. Sections were washed 2 × 5 min in TBS and treated at room temperature for 24 h with the primary antibody at the dilution indicated in Table 1. After a washing step of 2 × 5 min in TBS, sections treated with polyclonal anti-rabbit primary antibodies or monoclonal anti-mouse primary antibodies were incubated for 1 h with 1:200 biotinylated anti-rabbit immunoglobulins (Vector Labs, Burlingame, CA, USA) or with 1:200 biotinylated anti-mouse immunoglobulins (Vector Labs), respectively (Table 1). Finally, sections were treated for 1 h at room temperature with the streptavidin-biotin/horseradish peroxidase complex (Vectastain® ABC kit, Vector Labs, Burlingame, CA, USA) and then with a freshly prepared solution of 4 mg of 3,3′-diaminobenzidine tetrahydrochloride (Sigma-Aldrich, Saint Louis, MO, USA) in 10 mL of TBS containing 0.1 mL of 1% H_2O_2. After 15 min washing steps in running tap water, sections were counterstained for 10 min with Mayer's haematoxylin, de-hydrated, cleared in xylene, and mounted with Eukitt (Sigma-Aldrich, Saint Louis, MO, USA).

Since the presence of melanin in tissues, especially MAs, could result in a false positive reaction, a melanin bleaching protocol was used to remove melanin [34]. After re-hydration, one of two serial sections were treated with 0.5% H_2O_2 in 10 mM Tris/HCl pH 10.0 at 80 °C for 15 min prior of the endogenous peroxidase blocking step and the subsequent steps of the immunohistochemical protocol. Moreover, the following control protocols were performed: (1) incubation with phosphate-buffered saline (PBS) pH 7.4 instead of the primary antibody; (2) treatment with PBS instead of the secondary antibody; (3) melanin bleaching treatment prior of the incubation step with PBS instead of the primary antibody; (4) pre-adsorption of each antibody with the corresponding antigen (Table 2). All these procedures gave the expected results (Figure S1).

For lectin histochemistry, sections of the eel SB parasitized with *A. crassus* were de-paraffinized, re-hydrated and washed 2 × 5 min in TBS. Then, sections were treated for 20 min with 3% H_2O_2 in TBS, newly washed 2 × 5 min in TBS and incubated in a humid chamber for 3 h at room temperature with 10 µg/mL biotinylated lectin (Table 3) in 10 mM HEPES pH 7.5, 0.15 M NaCl, 0.08% sodium azide, and 0.1 mM $CaCl_2$. After a 2 × 5 min washing step in TBS, sections were treated with the Vectastain® ABC Kit (Vector Labs, Burlingame, CA, USA) for 1 h at room temperature and then washed 2 × 5 min in TBS. The reaction was developed with a freshly prepared diaminobenzidine solution activated with 0.1 mL of 1% H_2O_2. Then, sections were counterstained with Mayer's hematoxylin, de-hydrated, cleared in xylene, and mounted with Eukitt. The negative controls were performed by (1) an incubation step with the HEPES buffer without lectin; (2) treatment of sections with a solution of lectins and the relative specific sugars (Table 3) added at a concentration of 0.2 M. All these procedures removed the lectin reactivity.

Table 1. Antibodies used in this study, their specificity, working dilution, source and code.

Antibody Anti-	Host	Dilution	Source	Code
CD4	Rabbit	1:50	Biorbyt Ltd., Cambridge, UK	orb4830
Histamine	Rabbit	1:100	Novus Biologicals, Centennial, CO, USA	NBP2-45266
IgM	Mouse	1:50	Biorbyt Ltd., Cambridge, UK	orb510864
Interleukin-6	Mouse	1:25	Santa Cruz Biotechnology, Inc., Santa Cruz, CA, USA	sc-28343
Lysozyme	Mouse	1:50	Santa Cruz Biotechnology, Inc., Santa Cruz, CA, USA	sc-518012
NOS 2	Rabbit	1:10	Santa Cruz Biotechnology, Inc., Santa Cruz, CA, USA	sc-651
Universal-NOS	Rabbit	1:25	NeoMarkers Inc., Fremont, CA, USA	RB-9261-P
Serotonin	Rabbit	1:100	Sigma-Aldrich, Saint Louis, MO, USA	S5545
Serotonin	Rabbit	1:100	Novus Biologicals, Centennial, CO, USA	NB100-65218
TLR-2	Rabbit	1:100	Biorbyt Ltd., Cambridge, UK	orb573647
TNF-α	Rabbit	1:50	Abcam, Cambridge, UK	ab6671
Tryptase ξ	Mouse	1:50	Santa Cruz Biotechnology, Inc., Santa Cruz, CA, USA	sc-377427
Anti-Biotinylated Secondary Antibodies				
Anti-rabbit IgG	Goat	1:200	Vector Labs, Burlingame, CA, USA	BA-1000
Anti-mouse IgG	Goat	1:200	Vector Labs, Burlingame, CA, USA	BA-9200

Table 2. Blocking molecules used for the antibodies' pre-adsorption test.

Blocking Molecules	Source	Code
Histamine	Sigma-Aldrich, Saint Louis, MO, USA	59964
Neuronal-Nitric Oxide Synthase (NOS 1)	Santa Cruz Biotechnology, Inc., Santa Cruz, CA, USA	Sc-5302
inducible-Nitric Oxide Synthase (NOS 2)	Santa Cruz Biotechnology, Inc., Santa Cruz, CA, USA	sc-7271 P
Serotonin	Sigma-Aldrich, Saint Louis, MO, USA	14927
Toll-Like Receptor-2 (TLR-2)	Novus Biologicals, Centennial, CO, USA	NB100-56720PEP
Tryptase	Sigma-Aldrich, Saint Louis, MO, USA	T7063

Sections were examined and photographed using a digital camera (C-P20CC, 20 Mp, Optika, Bergamo, Italy) and image analysis software (Proview v.x64, Optika, Bergamo, Italy).

For transmission electron microscopy (TEM), numerous 7 × 7 mm pieces of infected and uninfected SB and intestine were fixed and embedded according to methods reported previously [21,32]. Ultra-thin sections (90 nm) of both organs were stained with 4% uranyl acetate solution in 50% ethanol and Reynold's lead citrate. A Hitachi H-800 (Tokyo, Japan) transmission electron microscope was used to examine stained sections of SB and intestines.

Table 3. Biotinylated lectins used in this study, their preferred binding carbohydrate specificities, and source code.

Acronym	Lectin	Species Source: Latin Name (Common Name)	Major Carbohydrate Specificity	Vector Laboratories Code
UEA I	Ulex europaeus agglutinin I	*Ulex europaeus* (gorse seed)	Fucose	B-1065
WGA	Wheat germ agglutinin	*Triticum vulgare* (wheat germ)	N-acetylglucosamine, sialic acid	B-1025

3. Results

From the swimbladders of 66 of 97 (68%) eels, a total of 480 adult specimens of nematode *A. crassus* were counted, and the intensity of infection ranged from 1 to 18 adult worms per SB (7.27 ± 0.43, mean ± SE). During autopsy, the SB without parasites had thin walls and appeared transparent; conversely, those with several worms inside were darker and less transparent. Upon excision of the parasitized SB, big and dark brownish worms within the lumen were visible to the naked eye (Figure 1a). In most parasitized swimbladders, the co-occurrence of very big gravid females and smaller specimens of *A. crassus* was noticed (Figure 1a).

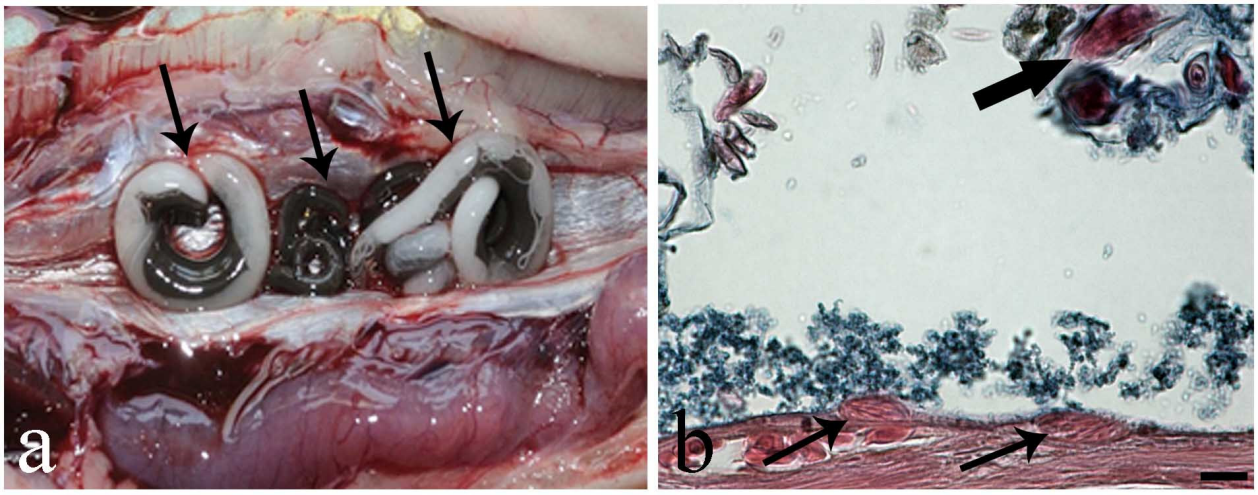

Figure 1. Photo after necropsy of *Anguilla anguilla* and photo from histological slide of the swimbladder. (**a**) Opened heavily infected swimbladder (SB) with big adult *Anguillicoloides crassus* (arrows) occupying the organ's lumen. (**b**) Histological section of *A. anguilla* swimbladder, two rodlet cells (arrows) within the epithelium of the infected (SB), note presence of rodlets inside the cells, thick arrow shows *A. crassus* larva, Alcian Blue/Haematoxylin and Eosin stain, scale bar = 20 µm.

Observations of histological sections showed considerable structural differences between infected and uninfected SB (Figure S2a); briefly, in several SBs harboring some *A. crassus*, the most remarkable change noticed was the proliferation of epithelial cells, giving the folds a papillose aspect (Figure S2b). In heavily infected SBs, dilation of blood vessels in the mucosal layer (Figure S2b), inflammation, and hemorrhages were frequent. Indeed, big adult *A. crassus* often occupied most of the luminal space of the organ, and the feeding activity of these worms provoked erosion of portions of the SB epithelium.

In parasitized SB, MAs and MCs were observed in the mucosal layer. Interestingly, in several heavily infected SB, RCs were the sole fish immune cells, encountered in the epithelium and close to the *A. crassus* (Figure 1b). Rodlet cells in parasitized SBs appeared as oval and crushed cells (Figure 1b) in comparison to long RCs from eel intestine. They had a distinctive cell cortex and inclusions called rodlets (Figure 1b). Macrophages appeared as big cells with an irregular shape and outline, and contained dark undefined dense bodies

in the cytoplasm (Figures 2 and 3). For Mas, a melanin bleaching protocol (see [34]) was followed on serial sections to remove melanin; this further step confirmed the occurrence of the MAs. Mast cells presented an elongated-ovoid shape and contained numerous polymorphic granules that displaced the nucleus to the cell periphery (Figure 2).

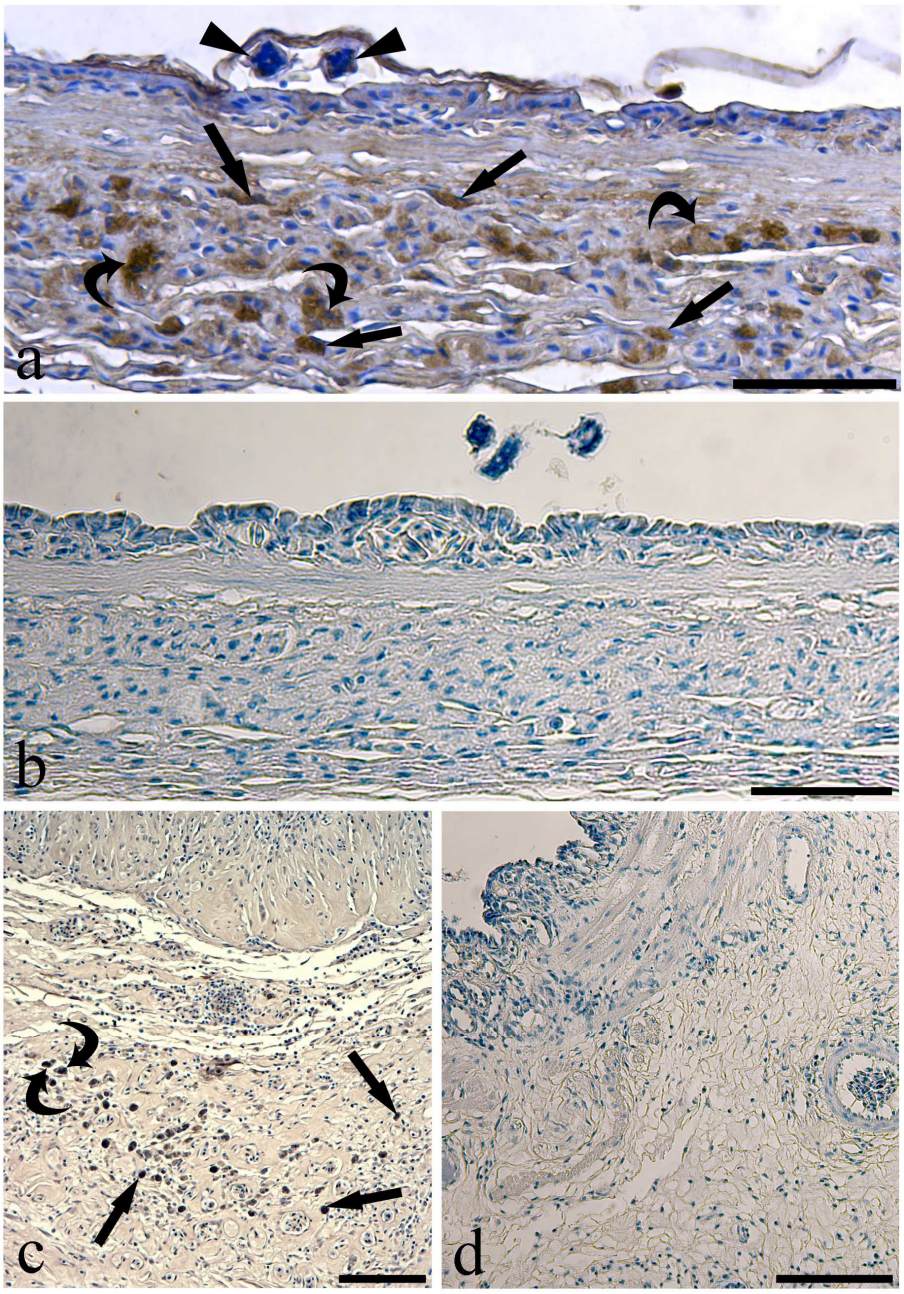

Figure 2. Micrographs of immunohistochemical reactions on sections of infected eel swimbladder. (**a**) Several mast cells (arrows) and presumable macrophages (curved arrows) in the mucosal layer immunoreactive to anti-histamine; see two pieces of a larva (arrowheads) covered by surfactant, scale bar = 50 μm. (**b**) The mucosal layer showed no immunoreactive cells when anti-histamine was pre-adsorbed with the blocking molecule, scale bar = 50 μm. (**c**) Mast cells (arrows) and presumable macrophage (curved arrow) scattered in the *tunica submucosa* positive to anti-serotonin, scale bar = 100 μm. (**d**) Pre-adsorption with anti-serotonin blocking molecule removed the reactivity appeared in the previous images of this figure, scale bar = 50 μm.

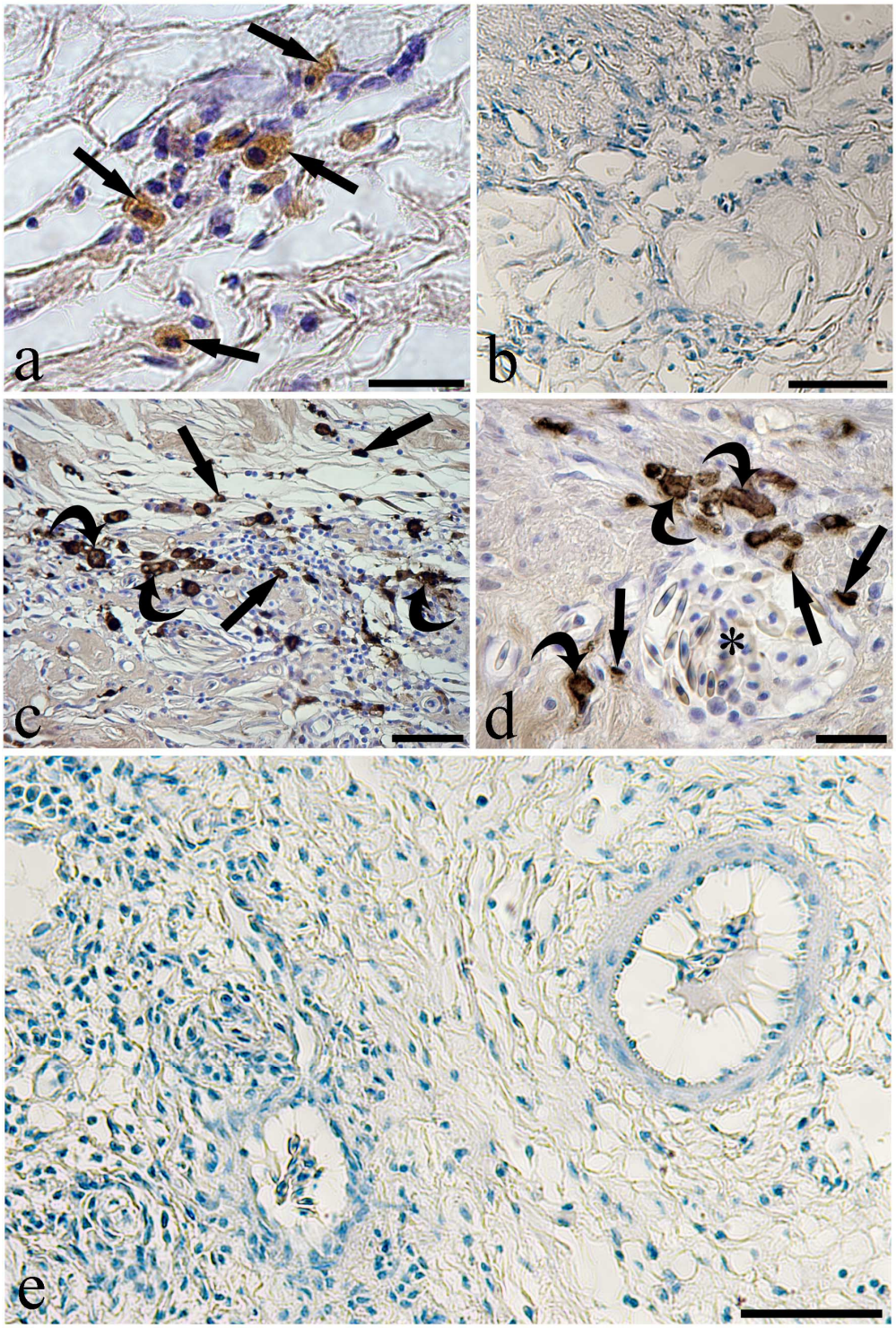

Figure 3. Micrographs of immunohistochemical reactions on sections of infected eel swimbladder. (**a**) Some mast cells (arrows) react to the anti-tryptase in the *tunica submucosa*, scale bar = 20 μm. (**b**) No immunoreactive cells are seen in the *tunica submucosa* when anti-tryptase was pre-adsorbed with its blocking peptide, scale bar = 100 μm. (**c**) A high number of mast cells (arrows) and presumable macrophages (curved arrows) positive to the anti-inducible-nitric oxide synthase (i-NOS) in the *tunica submucosa*, scale bar = 50 μm. (**d**) The high magnification shows mast cells (arrows) and presumable macrophages (curved arrows) close to a blood vessel full of erythrocytes (asterisk), scale bar = 20 μm. (**e**) The pre-absorption of anti-i-NOS with its blocking peptide removed the reactivity appeared in the previous images of this Figure, scale bar = 50 μm.

Within the thickness of the *tunica submucosa* of the infected SBs, several MCs were immunoreactive to the anti-histamine antibody (Figure 2a) as confirmed by the pre-adsorption test (Figure 2b). The antibody anti-serotonin detected MCs and presumable MAs scattered in the connective tissue of the *tunica submucosa* (Figure 2c,d). In the same tissue layer, immune cells reactive to the antibody anti-Tryptase (Figure 3a,b) were observed. In the infected SBs, a high number of presumable MAs were immunoreactive to the anti-i-NOS antibody (Figure 3c–e). The same anti-i-NOS revealed that MCs were located around blood vessels in the wall of the parasitized SBs (Figure 3d). Fewer MCs and presumable MAs immunoreactive to the above antibodies were observed in the uninfected SB (Figure S3). The antibodies anti-CD4, -immunoglobulin M, -interleukin-6, -lysozyme, and -tumor necrosis factor-α did not detect any cell components in the eel SB.

The anti-toll-like receptor-2 (TLR-2) antibody detected unusual epithelial funnel-shaped cells in the infected eel SB (Figure 4a). These cells were also present in sections pre-treated for the bleaching of melanin (Figure 4b). Notwithstanding, the same cells were not seen in sections pre-adsorbed with the blocking peptide (Table 2, Figure 4c), incubated without the anti-TLR-2, and pre-treated for the melanin bleaching (Figure 4d). The lectins WGA and UEA I (Table 3) un-marked and marked, respectively, the funnel-shaped cells of the SB epithelium (Figure 4e–g). Similar cells were observed at the ultrastructural level, showing a darker cytoplasm with some electron-dense spots in the upper region of the cell (Figure 4h).

In our examinations of eel intestine, histological sections of 15 fish revealed coccidians inside the enterocytes (Figure 5a–e); the parasite was never encountered in an epicellular position (see Figure 5b–e). Identification of the coccidian species was outside the scope of the present survey. Based on the size of the coccidians, their differentiation observed by TEM microscopy, and comparison with data on the stages of a coccidian found in *A. anguilla* in Molnar and Baska [17], two presumed stages were observed, specifically macrogamont (Figure 5a,c–e) and meront; both stages develop in a parasitophorous vacuole within the thickness of the epithelium. The meront in the host enterocyte appeared as a round globule with a diameter ranging from 5.98 to 8.26 µm (Figures 5b and S4c). The macrogamont was visible as a big, oval-round and compact globule with a diameter ranging from 12.24 to 15.40 µm (Figure 5a,c–e). In the epithelium, both meront and macrogamont were close to a cluster of very big RCs (Figure 5b–e). The coccidian moved toward the top of the epithelium and then entered the lumen after rupture of the thin membrane of the parasitophorous vacuole (Figure 5b–d). In sections of two eel intestines, we noticed the presence of very few oocysts with sporocysts inside (Figure S4a), and TEM observation revealed Stieda body and sub-Stieda in the apical part of the sporocyst (Figure S4b). Epithelial cell destruction and erosion of the intestinal folds were common. Figure 5e clearly shows the internal aspect of some well-developed macrogamonts and their close proximity and contact with several very big RCs. Moreover, within the connective tissue of the infected intestinal fold, some MCs in degranulation and near the coccidian were documented (Figure 5f). A low number of the RCs occurred in uninfected intestine (Figure S4d).

The RCs of the eel intestine showed an interesting immunoreactivity to the anti-universal NOS antibody (Table 1) at the cell apex (Figure 6). Differences in the extension of stained signals as well as stain intensity at the RC's apex were also noticed (Figure 6a); nevertheless, in the same section, very few RCs were unreactive (Figure 6a). The pre-adsorption of antibody anti-u-NOS with blocking peptides (Table 2) completely removed the reactivity on the RCs (Figure 6b).

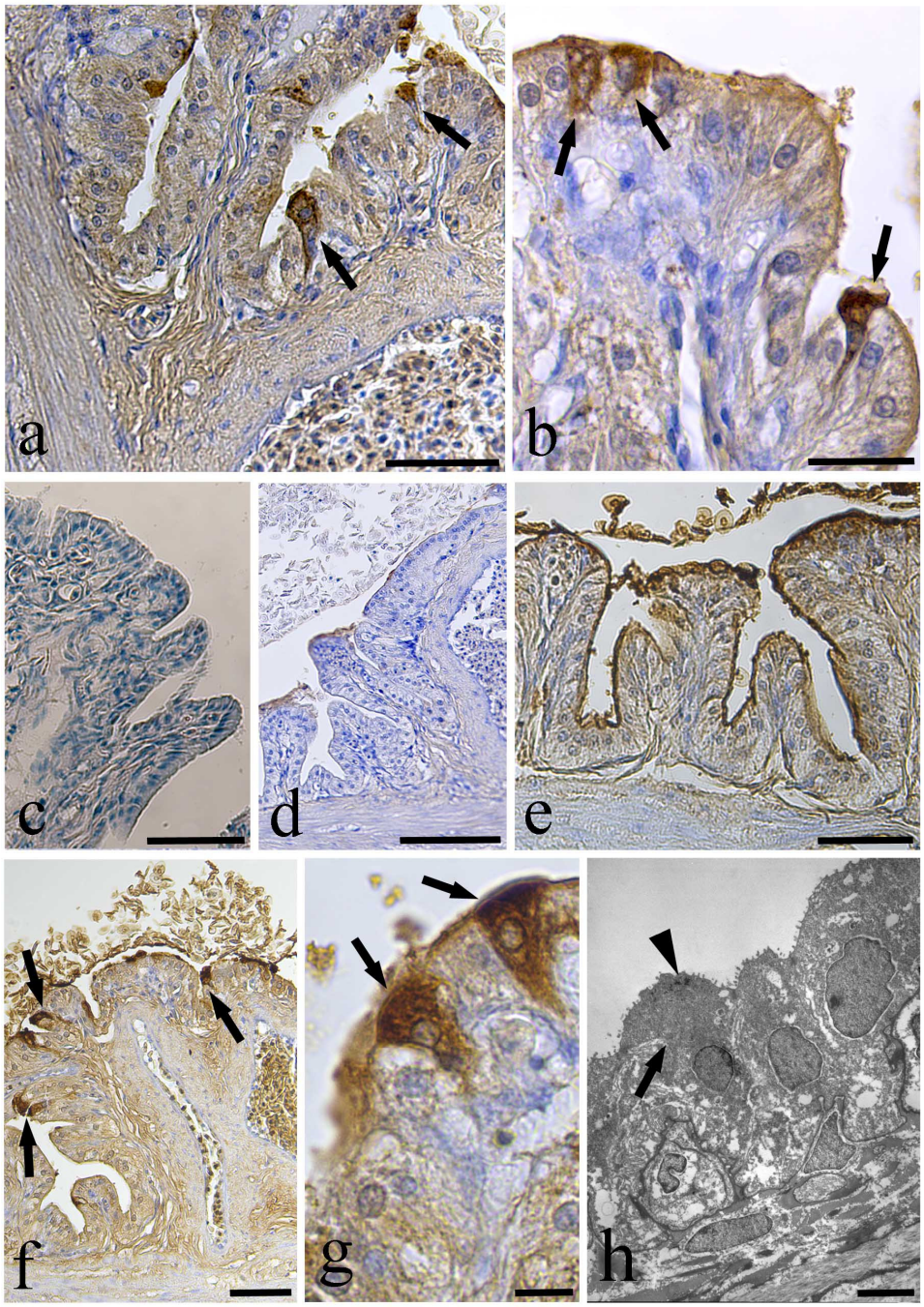

Figure 4. Anti-Toll-Like Receptor-2 (TLR-2) immunohistochemistry and lectin histochemistry on sections of the infected swimbladder. (**a**) Two epithelial funnel-shaped cells (arrows) immunoreactive to anti-TLR-2 antibody, scale bar = 50 µm. (**b**) After the melanin bleaching treatment, the anti-TLR-2 positive cells are visible (arrows), scale bar = 20 µm. (**c**) After pre-absorption test, no immunoreactive cells were evident in the swimbladder epithelium, scale bar = 50 µm. (**d**) No positive cells were noticed in the section of swimbladder treated for melanin bleaching and incubated without the anti-TLR-2, scale bar = 100 µm. (**e**) The test for lectin WGA showed no positive cells in the epithelium, scale bar = 50 µm. (**f**) The lectin UEA I marked the epithelial funnel-shaped cells (arrows) of the swimbladder, scale bar = 50 µm. (**g**) High magnification showing the funnel-shaped cells (arrows) reactive to the lectin UEA I, scale bar = 10 µm. (**h**) The transmission electron micrograph shows a funnel-shaped cell (arrow) with small dark dots near the cell apex (arrow head), scale bar = 5 µm.

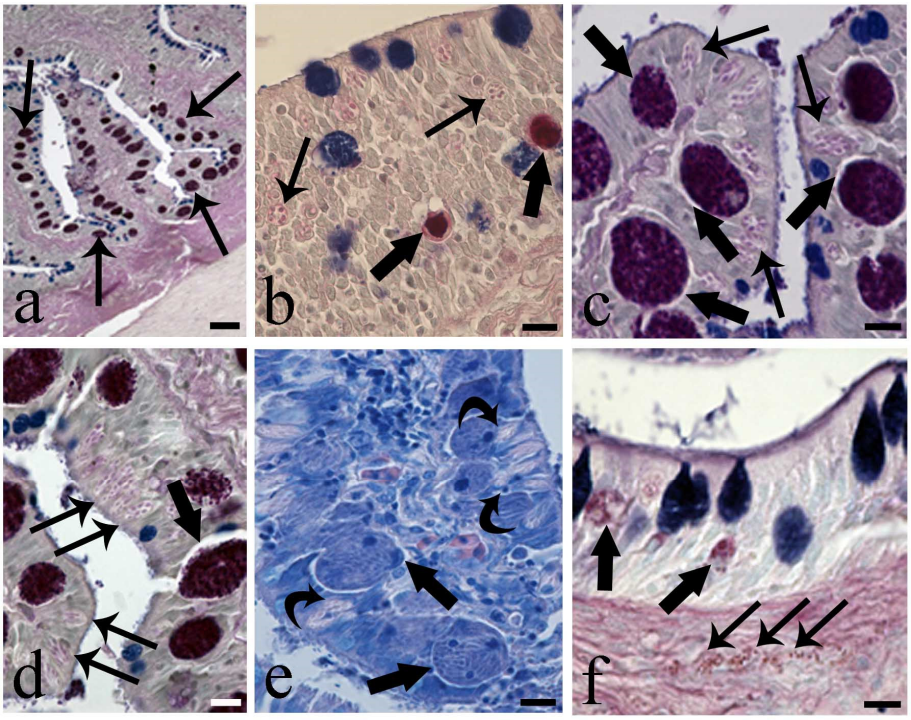

Figure 5. Micrographs of intestinal sections showing the presence of coccidians. (**a**) Low magnification of section of infected intestine of *Anguilla anguilla.* Numerous macrogamonts (arrows) within the enteric epithelial cells are visible, Alcian Blue and Periodic Acid Schiff's, AB/PAS stain, scale bar = 20 µm. (**b**) Two meronts (thick arrows) close to numerous rodlet cells (arrows), AB/PAS stain, scale bar = 10 µm. (**c**) Photo of the apical part of two adjacent villi, some macrogamonts near the top of the epithelium (thick arrows) and many big RCs (arrows) are visible, AB/PAS stain, scale bar = 10 µm. (**d**) High magnification of a macrogamont inside a parasitophorous vacuole (thick arrow); several big RCs (arrows) are evident, AB/PAS stain, scale bar = 10 µm. (**e**) Heavily infected enteric cells containing macrogamonts of coccidian parasite (thick arrows); curved arrows show contact between macrogamonts and RCs, Giemsa stain, scale bar = 10 µm. (**f**) Occurrence of two meronts (thick arrows) within the epithelium; some mast cells (arrows) in *tunica propria* can be seen, AB/PAS stain, scale bar = 10 µm.

Transmission electron microscopy of eel intestine harboring coccidians revealed that the parasite occupied the entire cytoplasm of the epithelial cell and displaced the nucleus to the marginal space of the cytoplasm and beneath the plasmalemma (Figure 7a). An increase in size of the coccidian induced the disintegration of the epithelial cells and the release of the parasite to the intestinal lumen (Figure 7a). The macrogamont contained several well-developed gametocytes (Figure 7a–c); each gametocyte had an evident euchromatic nucleus, many amylopectin granules in the cytoplasm (Figure 7c), well-developed rough endoplasmic reticulum, and some mitochondria (not shown). Figure 7c shows two gametocytes in the periphery of the macrogamont. The meront had some gametocytes in differentiation; their nuclei were disseminated in the periphery of the meront cytoplasm, and there was no distinct plasmalemma around each gametocyte and no amylopectin granules (see Figure S4c). In most of the 15 infected intestines, a cluster of very big RCs occurred close to the coccidian (Figure 7d). Fewer RCs were present in the uninfected eel intestine (Figure S4d).

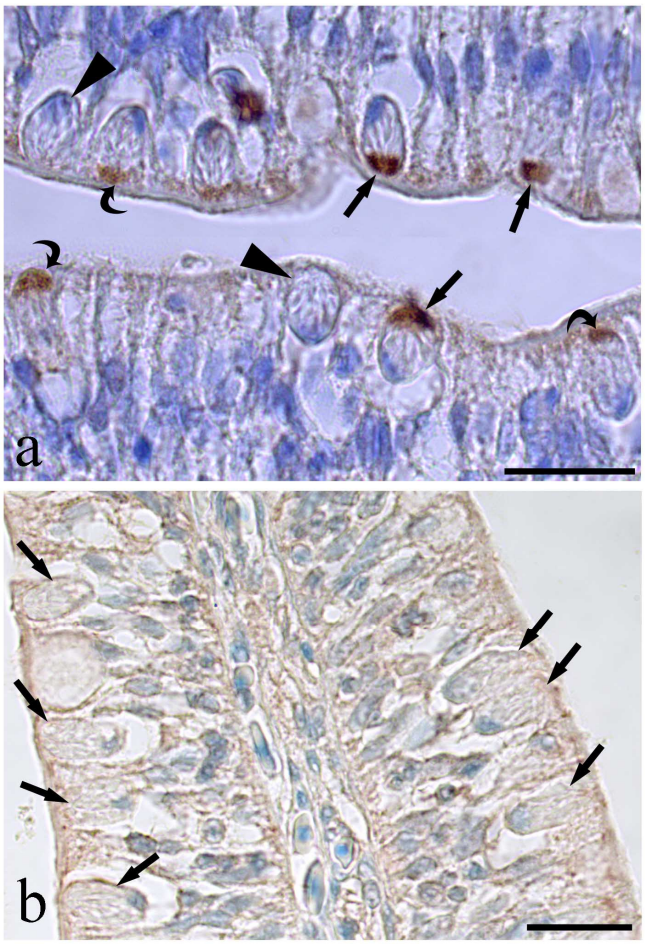

Figure 6. Photos of rodlet cells immunoreactive to the anti-universal-NOS in the infected eel intestine. (**a**) Several rodlet cells showing a positive reaction to the antibody only at their apex, some rodlet cells show a strong stain apex (arrows), others are faintly colored (curved arrows) and very few are unreactive (arrow heads), scale bar = 20 μm. (**b**) Image shows an epithelial area with high density of unreactive rodlet cells after the pre-absorbed test with a mix of neuronal-nitric oxide synthase and inducible-nitric oxide synthase, scale bar = 50 μm.

Rodlet cells were characterized by a distinctive cell cortex and conspicuous inclusions named rodlets (Figure 7d,e) with cortex thickness ranging from 0.6–0.9 μm. The rodlet cell nuclei were round, oval, or U-shaped with an irregular outline and occupied the basal portion of the cell (Figure 7d). Most often, the nuclei were characterized by randomly distributed zones of heterochromatin, also noticed in their periphery (Figure 7d). Frequently, mitochondria were observed as small and round and in the apex of the cell; at the apex of the cell, some translucent vesicles were encountered. Club-shaped rodlets contained electron-opaque inclusions and were arranged so that the head of the club was oriented toward the basal nucleus and the narrow part or core toward the apex-opening pole of the rodlet cell (Figure 7d,e). In the eel intestine, desmosomes between RCs and with surrounding epithelial cells were found commonly.

With reference to SBs infected with *A. crassus*, MCs and MAs were noticed in the mucosal layer and sometimes among the epithelial cells; conversely, RCs in variable numbers were seen only in organ epithelium (Figure 7f) and close to the *A. crassus* (Figure 7g). Remarkable differences were noticed between RCs in the SB and those in the intestine. In SBs, they were smaller, oval, and with fewer rodlets in the cytoplasm (Figure 7f,g). Herein, RCs displayed signs of degeneration, such as cytoplasmic vacuolization, cortex deformation, and absence or paucity of organelles. Moreover, their rodlets often were rarefied, very electron-dense and seldom were cores present (Figure 7f,g).

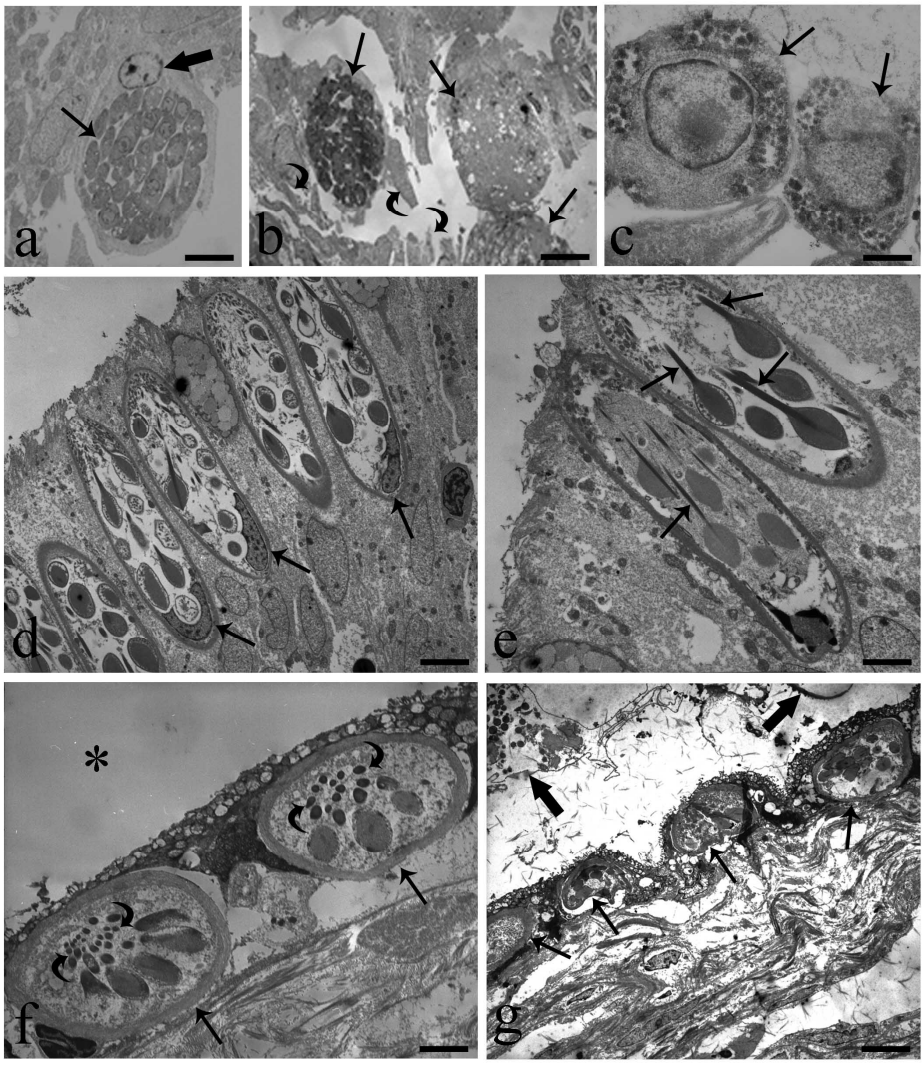

Figure 7. Transmission electron micrographs of *A. anguilla*-infected intestine and swimbladder. (**a**) Macrogamont (arrow) inside the cytoplasm of an enteric cell; note host cell nucleus (thick arrow) in the periphery of the cytoplasm, scale bar = 3.5 µm. (**b**) Macrogamonts (arrows) leaving the intestinal villi by destruction of the enteric cells; residue of cells (curved arrows) in the lumen are visible, scale bar = 6 µm. (**c**) Photo shows the periphery of the macrogamont; two gametocytes (arrows) are evident, scale bar = 1 µm. (**d**) Cluster of big RCs in intestinal epithelium very close to coccidian; basal position of nuclei (arrows) is visible, scale bar = 4 µm. (**e**) Image shows typical club-shape rodlets and their well-developed cores (arrows) inside intestinal RCs, scale bar = 2.5 µm. (**f**) Two oval shape rodlet cells (arrows) in infected SB epithelium; SB lumen (*), note less number of rodlets and sections of their cores (curved arrows), scale bar = 2.3 µm. (**g**) Four rodlet cells (arrows) in SB epithelium are visible; thick arrows show portion of parasites in SB lumen. Differences in shape and size of SB rodlet cells with those of the intestine (Figure 7d,e) are appreciable, scale bar = 5.8 µm.

4. Discussion

Anguilla anguilla is one of the most important warm fish species cultured in several European countries. Eels are euryhaline fish with a very complex life cycle. For the European eel, the life cycle starts in the Sargasso Sea. The eels leave this spawning area as leptocephalus; at the coast, they reach glass eel stage, then elver stage [35].

Over 68% of the 97 SBs of the eels from Lake Trasimeno harbored the nematode *A. crassus*. The following pathological alterations in eel SB are due to *A. crassus*: increase in the thickness of the SB wall, lesion to the epithelium, dilation of blood vessels, hemorrhaging, fibrosis, occurrence of granulocytes and MAs around encysted nematode larvae, infiltration

of inflammatory cells, and decrease in SB elasticity [2,4]. It has been suggested that *A. crassus* alters the cellular and humoral immune response and physiological condition of the eel SB [4,5].

The mucosal immune system of fish is highly efficient and plays a critical role in resisting various pathogens [10,24]. The role of the mucosal immune response of European eels in a bacterial challenge was detailed in a recent paper by Conforto et al. [11]. Several records were published on the cellular immune response of eel SB infected with *A. crassus*; MAs and granulocytes around nematode larvae in the wall of different organs were commonly noticed [4,9,13]. In the mucosal layer of infected SBs, two very important components of the innate immune system, namely MCs and MAs, frequently were encountered. There is a dearth of records on the co-presence of MCs and MAs in the epithelium of the infected organs of fish; a short insight on roles of above immune cells will be provided.

With reference to the MCs, in fish as in other vertebrates they are strategically placed at perivascular sites [36]. Fish MCs migrate to infection sites [9,37], where they launch a first line of defense by releasing the contents of secretory granules, including powerful molecules such as histamine, piscidins, α-N-acetyl-galactosamine, and serotonin [26,38].

The teleost macrophage populations have been the best studied and shown to rapidly kill pathogens through phagocytosis [39]. MAs are active in immune defenses and found in over 130 fish species. The feeding activity of *A. crassus* damages the epithelial cells of the SB; thus, it is reasonable to believe intraepithelial MAs are necessary to phagocytose the residues of damaged cells. Several MCs and MAs were immunoreactive to anti-histamine and -serotonin antibodies. In vertebrates, the biogenic amines histamine and serotonin are the most important mast cell mediators [20,40]. In fish, histamine was first demonstrated by Mulero et al. [21]; later, it was noticed in the MCs of the pike *Esox lucius*, parasitized with an acanthocephalan [23], and in the MAs of the mullet *Chelon ramada*, infected with the myxozoan [22]. The early step in inflammation is the degranulation of the MCs with the release of histamine [20]. Our data on the occurrence of histamine in the immune cells of the eel's infected SB is further evidence of its role in inflammation. In this study, several MCs and presumable MAs immunoreactive to two different anti-serotonin antibodies were observed in the *tunica submucosa* of the infected SBs. The involvement of serotonin in the inflammatory response to pathogens were reviewed by Wang et al. [40].

Tryptase was detected in the MCs of teleosts [41] and elasmobranchs [33]. In the *tunica submucosa* of the eel's infected SB, clusters of MCs immunoreactive to anti-tryptase antibody were observed. Tryptase is the main type of serine protease stored in mast cell granules and highly conserved among vertebrates [42]. In mammals, tryptase is involved in the recruitment of granulocytes, in the epithelial repairing process, as well as in the activation of MCs themselves [26]. Nevertheless, despite the importance of tryptase in vertebrate immunology, little is known about this enzyme in fish granulocytes [26,33].

Molecules of nitric oxide (NO) are produced by the catalysis of L-arginine by a family of nitric oxide synthases (NOS) that includes two constitutive, neuronal and endothelial, and one inducible-NOS (i-NOS) [43]. In fish, i-NOS is synthesized primarily in MAs and MCs [22,29,44]. It was also found in the gill mucous cells of parasitized *Abramis brama* [45] and in the RCs of different fish species [29,37]. In the infected SBs of eels, the presence of MCs and presumable MAs containing i-NOS confirms the role of NO in the inflammatory mechanisms against pathogens [22].

In the epithelium of the parasitized SBs, many funnel-shaped cells were detected by the anti-TLR-2 antibody, especially when a high number of adult worms occurred in the lumen. The role of TLRs is the recognition of substances secreted by invading organisms, called the "pathogen-associated molecular pattern" (PAMP). The detection of PAMP results in an activation of MAs, dendritic cells and other types of immune cells to produce cytokines and various factors, which in turn induce other immune cells by autocrine/paracrine signals [27,46]. In vertebrates, TLR-2 recognizes molecular components of Gram-positive bacteria [47] and were detected in different organs of several fish species [46]. In carp, TLR-2 was reported to sense glycosyl-phosphatidyl-inositol from parasites [48]. In fact, the TLRs'

detection of PAMP induces an innate immune response against metazoan parasites [49], and TLR-2 expression increases with inflammation [50]. Several studies in teleost fish reported the involvement of TLRs in the immune defense against parasites [49,51]. The anti-TLR-2-immunoreactive funnel-shaped cells found in the parasitized eel SBs very closely resemble mammalian M cells [52]. Fuglem et al. [53] showed the presence of epithelial M-like cells in the intestine of Atlantic salmon. These cells were identified by the presence of their rich fucose content, detected by the lectin UEA I and the absence of reactivity to the lectin WGA, which revealed the presence of N-Acetylglucosamine and sialic acid residues [52]. Herein, we found the same lectin reactivity to the anti-TLR-2 in the funnel-shaped cells of the SB; this finding might suggest their possible role as antigen sampling cells in the parasitized SB.

In the intestine of 15 eels, macrogamont and meront stages of a coccidian were observed. The protozoans were close to clusters of RCs (Figure 4b–e). Several types of intestinal coccidian have been described based on their location and life cycle [14,17,54]. Accounts were published on coccidians of fishes from different regions of the world [54]. Papers on the pathogenicity of coccidians in fish intestine with necrosis and sloughing of epithelium was mentioned in [54,55]. With regard to the eels' coccidians, the occurrence of *Eimeria anguillae* in eels appeared in Molnar and Hanek [56]. *Epiemeria anguillae* was encountered in *A. anguilla* in different regions of the Europe [17]. In the present survey, the position of the coccidians in the intestinal epithelium was intracellular and differs from the epicellular position reported for *Epiemeria anguillae* in the same host by Molnar and Baska [17]. There is no agreement among authors concerning the virulence of fish intestinal coccidiosis. A lack of a clinical sign and a normal condition of fish was mentioned in Molnar et al. [57], whereas a significant health threat to young bluegills was supported in Pasnik et al. [55]. It was suggested that fish affected by coccidiosis are more susceptible to bacterial infection [54].

The RCs were the only immune cells in the epithelium of infected SBs as well as in that of intestine with coccidiosis; in both organs, the RCs were near the worm and protozoan. To shed more light on the functions of RCs, it is desirable to discover the nature of their contents. It was reported that RCs in gills harboring an ectoparasite were immunoreactive to the antimicrobial peptide piscidin-1 [58]. Indeed, RCs were shown to be immunoreactive to α-Melanocytes-Stimulating Hormone, and it was postulated that the above cells are subject to endocrine regulation, similar to leukocytes [59]. The presence of antimicrobial peptides and cytokines in the RCs support their defensive role as components of the fish innate immune system [9,29,37,60].

In this study, the use of a different antibody (universal-NOS from NeoMarkers, Fremont, CA, USA) was able to detect each peptide of the NOS family and marked RCs at their apical region. An accumulation of tropomyosin at the apical tip of the RCs was mentioned in [30]. Tropomyosin is a component of the contraction system in different cells and tissues [31,32]. The molecules of tropomyosin regulate the Ca^{2+}-dependent interaction of myosin heads with actin myofilaments [32]. In human lung, the vasodilation of arteries was induced by neurotrophins via increased NO production in a pathway involving tropomyosin-related kinase receptors and endothelial-NOS [61]. Moreover, cardiac muscle treated with reactive nitrogen species increased force production [62]. An experimental study suggested a direct myofilament sensibilization to Ca^{2+} from the nitrogen species [31]. The presence of NOS in the apex of the RCs with a high amount of tropomyosin [30] was thought to support the NO involvement in the contractile activity of the filaments. Therefore, it is reasonable to presume that co-occurrence of the NOS and tropomyosin at the apex of the RCs could be related to the cell-opening mechanism followed by the ejection of their contents.

This study provides further evidence on the role of the RCs and other immune cells against *A. crassus* in SB and on the intense response of the RCs to a coccidian in the eel intestine. Rodlet cells are enigmatic cells found only in teleosts that react against parasites as inflammatory cells. Thus, more immunohistochemical investigations are needed in the

search for links between RCs and other fish immune cells and RC contents. Herein, the immunohistochemical methods revealed for the first time the presence of anti-NOS at the RC's apical region. This result might shed light on the unknown opening mechanism of these cells. The present study was designed to begin an assessment on the immunoreactivity of MCs, MAs and RCs to 12 antibodies, of which most are involved in the host inflammatory response against pathogen parasites. Given the relative importance of innate immunity in fish and the magnitude of economic loss in farmed and wild fish as a consequence of disease and parasites, this area deserves considerable attention and support. It is hoped that the information provided by this paper will spur more research.

Supplementary Materials: The following supporting information can be downloaded at: https://www.mdpi.com/article/10.3390/fishes8020066/s1, Figure S1: Negative control sections of a parasitized swimbladder of *Anguilla anguilla*. Figure S2: Histological sections of uninfected and infected swimbladders of *Anguilla anguilla*. Figure S3. Immunohistochemical reactions on uninfected sections of the *Anguilla anguilla* swimbladder. Figure S4. Light and electron microscopic figures of intestine of *Anguilla anguilla* infected with coccidian.

Author Contributions: Conceptualization, B.S.D.; methodology, B.S.D. and G.B.; investigation, B.S.D., M.L., A.C. and G.B.; data curation, B.S.D., M.O. and G.B.; funding acquisition, B.S.D. and G.C.; writing—original draft preparation, B.S.D.; writing—review and editing, M.O. and G.B. All authors have read and agreed to the published version of the manuscript.

Funding: This work was supported in part by local grants from the University of Ferrara to B. Sayyaf Dezfuli (FAR 2021), and by grants from the Project LIFEEL—LIFE19 NAT/IT/000851 to G. Castaldelli—Urgent measures in the Eastern Mediterranean for the long-term conservation of endangered European eel (*Anguilla anguilla*).

Institutional Review Board Statement: This study was conducted in accordance with the guidelines of the Declaration of Helsinki and national law (D.L. 4 March 2014, n. 26), and was approved by Ferrara University Ethical Committee (TLX n. 2/2018).

Data Availability Statement: Not applicable.

Acknowledgments: We thank B.J. Maynard, Colorado State University, for the English revision of the MS.

Conflicts of Interest: The authors have no conflict of interest to declare for this research.

References

1. Pelster, B. Swimbladder function and the spawning migration of the European eel *Anguilla anguilla*. *Front. Physiol.* **2015**, *5*, 486. [CrossRef] [PubMed]
2. Lefebvre, F.; Wielgoss, S.; Nagasawa, K.; Moravec, F. On the origin of *Anguillicoloides crassus*, the invasive nematode of anguillid eels. *Aquat. Invasions* **2012**, *7*, 443–453. [CrossRef]
3. Sayyaf Dezfuli, B.; Maestri, C.; Lorenzoni, M.; Carosi, A.; Maynard, B.J.; Bosi, G. The impact of *Anguillicoloides crassus* (Nematoda) on European eel swimbladder: Histopathology and relationship between neuroendocrine and immune cells. *Parasitology* **2021**, *148*, 612–622. [CrossRef] [PubMed]
4. Knopf, K. The swimbladder nematode *Anguillicola crassus* in the European eel *Anguilla anguilla* and the Japanese eel *Anguilla japonica*: Differences in susceptibility and immunity between a recently colonized host and the original host. *J. Helminthol.* **2006**, *80*, 129–136. [CrossRef]
5. Sures, B.; Knopf, K.; Kloas, W. Induction of stress by the swimbladder nematode *Anguillicola crassus* in European eels, *Anguilla anguilla*, after repeated experimental infection. *Parasitology* **2001**, *123*, 179–184. [CrossRef]
6. Jacoby, D.M.P.; Casselman, J.M.; Crook, V.; DeLucia, M.B.; Ahn, H.; Kaifu, K.; Kurwie, T.; Sasal, P.; Silfvergrip, A.M.C.; Smith, K.G.; et al. Synergistic patterns of threat and the challenges facing global anguillid eel conservation. *Glob. Ecol. Conserv.* **2015**, *4*, 321–333. [CrossRef]
7. Maizels, R.M. Regulation of immunity and allergy by helminth parasites. *Allergy* **2020**, *75*, 524–534. [CrossRef]
8. Jackson, J.A.; Friberg, I.M.; Little, S.; Bradley, J.E. Review series on helminths, immune modulation and the hygiene hypothesis: Immunity against helminths and immunological phenomena in modern human populations: Coevolutionary legacies? *Immunology* **2009**, *126*, 18–27. [CrossRef]
9. Sayyaf Dezfuli, B.; Giari, L.; Bosi, G. Survival of metazoan parasites in fish: Putting into context the protective immune responses of teleost fish. *Adv. Parasitol.* **2021**, *112*, 77–132. [CrossRef]

10. Alvarez-Pellitero, P. *Mucosal Intestinal Immunity and Response to Parasite Infections in Ectothermic Vertebrates*; Nova Science Publishers, Inc.: New York, NY, USA, 2011; 108p.
11. Conforto, E.; Vilchez-Gomez, L.; Parrinello, D.; Parisi, M.G.; Esteban, M.A.; Cammarata, M.; Guardiola, F.A. Role of mucosal immune response and histopathological study in European eel (*Anguilla anguilla* L.) intraperitoneal challenged by *Vibrio anguillarum* or *Tenacibaculum soleae*. *Fish Shellfish. Immunol.* **2021**, *114*, 330–339. [CrossRef]
12. Holtzinger, A.; Evans, T. Gata4 regulates the formation of multiple organs. *Development* **2005**, *132*, 4005–4014. [CrossRef] [PubMed]
13. Würtz, J.; Taraschewski, H. Histopathological changes in the swimbladder wall of the European eel *Anguilla anguilla* due to infections with *Anguillicola crassus*. *Dis. Aquat. Org.* **2000**, *39*, 121–134. [CrossRef] [PubMed]
14. Dyková, I.; Lom, J. *Histopathology of Protistan and Myxozoan Infections in Fishes, an Atlas*; Academia Press: Prague, Czech Republic, 2007.
15. Kristmundsson, A.; Hansen, H.; Alarcon, M.; Freeman, M.A. An eimerid apicomplexan causing pathology in wild and farmed lumpfish, *Cyclopterus lumpus*. *Bull. Eur. Ass. Fish Pathol.* **2018**, *38*, 213–221.
16. Matsche, M.A.; Blazer, V.S.; Mazik, P.M. Seasonal development of the coccidian parasite *Goussia bayae* and hepatobiliary histopathology in white perch *Morone americana* from Chesapeake Bay. *Dis. Aquat. Org.* **2019**, *134*, 113–135. [CrossRef]
17. Molnár, K.; Baska, F. Light and electron microscopic studies on *Epieimeria anguillae* (Léger & Hollande, 1922), a coccidium parasitizing the European eel, *Anguilla anguilla* L. *J. Fish Dis.* **1986**, *9*, 99–110. [CrossRef]
18. Benajiba, M.H.; Marques, A.; Lom, J.; Bouix, G. Ultrastructure and sporogony of *Eimeria* (syn. *Epieimeria*) *anguillae* (Apicomplexa) in the eel (*Anguilla anguilla*). *J. Eukaryot. Microbiol.* **1994**, *41*, 215–222. [CrossRef]
19. Hine, P.M. *Eimeria anguillae* Léger & Hollande, 1922 parasitic in New Zealand eels. *N. Z. J. Mar. Freshw. Res.* **1975**, *9*, 239–243. [CrossRef]
20. Buhner, S.; Schemann, M. Mast cell-nerve axis with a focus on the human gut. *Biochim. Biophys. Acta* **2012**, *1822*, 85–92. [CrossRef]
21. Mulero, I.; Sepulcre, M.P.; Meseguer, J.; García-Ayala, A.; Mulero, V. Histamine is stored in mast cells of most evolutionarily advanced fish and regulates the fish inflammatory response. *Proc. Natl. Acad. Sci. USA* **2007**, *104*, 19434–19439. [CrossRef]
22. Sayyaf Dezfuli, B.; Castaldelli, G.; Tomaini, R.; Manera, M.; DePasquale, J.A.; Bosi, G. Challenge for macrophages and mast cells of *Chelon ramada* to counter an intestinal microparasite, *Myxobolus mugchelo* (Myxozoa). *Dis. Aquat. Org.* **2020**, *138*, 171–183. [CrossRef]
23. Sayyaf Dezfuli, B.; Giari, L.; Lorenzoni, M.; Carosi, A.; Manera, M.; Bosi, G. Pike intestinal reaction to *Acanthocephalus lucii* (Acanthocephala): Immunohistochemical and ultrastructural surveys. *Parasite Vector* **2018**, *11*, 424. [CrossRef] [PubMed]
24. Sayyaf Dezfuli, B.; DePasquale, J.A.; Castaldelli, G.; Giari, L.; Bosi, G. A fish model for the study of the relationship between neuroendocrine and immune cells in the intestinal epithelium: *Silurus glanis* infected with a tapeworm. *Fish Shellfish Immunol.* **2017**, *64*, 243–250. [CrossRef] [PubMed]
25. Ceccotti, C.; Giaroni, C.; Bistoletti, M.; Viola, M.; Crema, F.; Terova, G. Neurochemical characterization of myenteric neurons in the juvenile gilthead sea bream (*Sparus aurata*) intestine. *PLoS ONE* **2018**, *13*, e0201760. [CrossRef]
26. Da Silva, W.F.; Simões, M.J.; Gutierre, R.C.; Egami, M.I.; Santos, A.A.; Antoniazzi, M.M.; Sasso, G.R.; Ranzani-Paiva, M.J.T. Special dyeing, histochemistry, immunohistochemistry and ultrastructure: A study of mast cells/eosinophilic granules cells (MCs/EGC) from *Centropomus parallelus* intestine. *Fish Shellfish Immunol.* **2017**, *60*, 502–508. [CrossRef]
27. Korenaga, H.; Nagamine, R.; Sakai, M.; Kono, T. Expression profile of cytokine genes in *Fugu* monocytes stimulated with TLR agonists. *Int. Immunopharmacol.* **2013**, *17*, 390–399. [CrossRef] [PubMed]
28. Mahla, R.S.; Reddy, M.C.; Prasad, D.V.R.; Kumar, H. Sweeten PAMPs: Role of sugar complexed PAMPs in innate immunity and vaccine biology. *Front. Immunol.* **2013**, *4*, 248. [CrossRef] [PubMed]
29. Bosi, G.; DePasquale, J.A.; Manera, M.; Castaldelli, G.; Giari, L.; Sayyaf Dezfuli, B. Histochemical and immunohistochemical characterization of rodlet cells in the intestine of two teleosts, *Anguilla anguilla* and *Cyprinus carpio*. *J. Fish Dis.* **2018**, *41*, 475–485. [CrossRef]
30. DePasquale, J.A. Tropomyosin and alpha-actinin in teleost rodlet cells. *Acta Zool.* **2020**, *102*, 323–332. [CrossRef]
31. Gao, W.D.; Murray, C.I.; Tian, Y.; Zhong, X.; DuMond, J.F.; Shen, X.; Stanley, B.A.; Foster, D.B.; Wink, D.A.; King, S.B.; et al. Nitroxyl-mediated disulfide bond formation between cardiac myofilament cysteines enhances contractile function. *Circ. Res.* **2012**, *111*, 1002–1011. [CrossRef]
32. Lehman, W.; Morgan, K.G. Structure and dynamics of the actin-based smooth muscle contractile and cytoskeletal apparatus. *J. Muscle Res. Cell. Motil.* **2012**, *33*, 461–469. [CrossRef]
33. Sayyaf Dezfuli, B.; Manera, M.; Bosi, G.; Merella, P.; DePasquale, J.A.; Giari, L. Intestinal granular cells of a cartilaginous fish, thornback ray *Raja clavata*: Morphological characterization and expression of different molecules. *Fish Shellfish Immunol.* **2018**, *75*, 172–180. [CrossRef] [PubMed]
34. Chung, J.Y.; Choi, J.; Sears, J.D.; Ylaya, K.; Perry, C.; Choi, C.H.; Hong, S.-M.; Cho, H.; Brown, K.M.; Hewitt, S.M. A melanin-bleaching methodology for molecular and histopathological analysis of formalin-fixed paraffin-embedded tissue. *Lab. Investig.* **2016**, *96*, 1116–1127. [CrossRef] [PubMed]
35. Tesch, F.W. *The Eel*, 5th ed.; Wiley-Blackwell: Chichester, UK, 2008.
36. Secombes, C.J.; Ellis, A.E. The immunology of teleosts. In *Fish Pathology*; Roberts, R.J., Ed.; Blackwell Publishing: Chicester, UK, 2012; Volume 4, pp. 144–166.

37. Sayyaf Dezfuli, B.; Pironi, F.; Maynard, B.J.; Simoni, E.; Bosi, G. Rodlet cells, fish immune cells and a sentinel of parasitic harm in teleost organs. *Fish Shellfish Immunol.* **2022**, *121*, 516–534. [CrossRef] [PubMed]
38. Dezfuli, B.S.; Bo, T.; Lorenzoni, M.; Shinn, A.P.; Giari, L. Fine structure and cellular responses at the host-parasite interface in a range of fish-helminth systems. *Vet. Parasitol.* **2015**, *208*, 272–279. [CrossRef] [PubMed]
39. Rieger, A.M.; Hall, B.E.; Barreda, D.R. Macrophage activation differentially modulates particle binding, phagocytosis and downstream antimicrobial mechanisms. *Dev. Comp. Immunol.* **2010**, *34*, 1144–1159. [CrossRef] [PubMed]
40. Wang, S.J.; Sharkey, K.A.; McKay, D.M. Modulation of the immune response by helminths: A role for serotonin? *Biosci. Rep.* **2018**, *38*, BSR20180027. [CrossRef]
41. Da'as, S.; Teh, E.M.; Dobson, J.T.; Nasrallah, G.K.; McBride, E.R.; Wang, H.; Neuberg, D.S.; Marshall, J.S.; Lin, T.-J.; Berman, J.N. Zebrafish mast cells possess an FcεRI-like receptor and participate in innate and adaptive immune responses. *Dev. Comp. Immunol.* **2011**, *35*, 125–134. [CrossRef]
42. McNeil, H.P.; Adachi, R.; Stevens, R.L. Mast cell-restricted tryptases: Structure and function in inflammation and pathogen defense. *J. Biol. Chem.* **2007**, *282*, 20785–20789. [CrossRef]
43. Andreakis, N.; D'Aniello, S.; Albalat, R.; Patti, F.P.; Garcia-Fernandez, J.; Procaccini, G.; Sordino, P.; Palumbo, A. Evolution of the nitric oxide synthase family in metazoans. *Mol. Biol. Evol.* **2011**, *28*, 163–179. [CrossRef]
44. Losada, A.P.; Bermúdez, R.; Faílde, L.D.; Quiroga, M.I. Quantitative and qualitative evaluation of iNOS expression in turbot (*Psetta maxima*) infected with *Enteromyxum scophthalmi*. *Fish Shellfish Immunol.* **2012**, *32*, 243–248. [CrossRef]
45. Dezfuli, B.S.; Giari, L.; Konecny, R.; Jaeger, P.; Manera, M. Immunohistochemistry, ultrastructure and pathology of gills of *Abramis brama* from Lake Mondsee, Austria, infected with *Ergasilus sieboldi* (Copepoda). *Dis. Aquat. Org.* **2003**, *53*, 257–262. [CrossRef] [PubMed]
46. Lee, P.; Zou, J.; Holland, J.W.; Martin, S.A.; Collet, B.; Kanellos, T.; Secombes, C.J. Identification and characterisation of TLR18-21 genes in Atlantic salmon (*Salmo salar*). *Fish Shellfish Immunol.* **2014**, *41*, 549–559. [CrossRef] [PubMed]
47. Schroder, N.W.; Morath, S.; Alexander, C.; Hamann, L.; Hartung, T.; Zähringer, U.; Göbel, U.B.; Weber, J.R.; Schumann, R.R. Lipoteichoic acid (LTA) of *Streptococcus pneumoniae* and *Staphylococcus aureus* activates immune cells via Toll-like receptor (TLR)-2, lipopolysaccharide binding protein (LBP), and CD14, whereas TLR-4 and MD-2 are not involved. *J. Biol. Chem.* **2003**, *278*, 15587–15594. [CrossRef] [PubMed]
48. Ribeiro, C.M.; Hermsen, T.; Taverne-Thiele, A.J.; Savelkoul, H.F.; Wiegertjes, G.F. Evolution of recognition of ligands from Gram-positive bacteria: Similarities and differences in the TLR2-mediated response between mammalian vertebrates and teleost fish. *J. Immunol.* **2010**, *184*, 2355–2368. [CrossRef] [PubMed]
49. Aguirre-García, M.M.; Rojas-Bernabé, A.; Gómez-García, A.P.; Escalona-Montaño, A.R. TLR-mediated host immune response to parasitic infectious diseases. In *Toll-Like Receptors*; Rezaei, N., Ed.; IntechOpen: London, UK, 2019. [CrossRef]
50. Hausmann, M.; Kiessling, S.; Mestermann, S.; Webb, G.; Spöttl, T.; Andus, T.; Schölmerich, J.; Herfarth, H.; Ray, K.; Falk, W.; et al. Toll-like receptors 2 and 4 are upregulated during intestinal inflammation. *Gastroenterology* **2002**, *122*, 1987–2000. [CrossRef]
51. Zhao, F.; Li, Y.W.; Pan, H.J.; Shi, C.B.; Luo, X.C.; Li, A.X.; Wu, S.-Q. Expression profiles of toll-like receptors in channel catfish (*Ictalurus punctatus*) after infection with *Ichthyophthirius multifiliis*. *Fish Shellfish Immunol.* **2013**, *35*, 993–997. [CrossRef]
52. Jang, H.M.; Kweon, M.-N.; Iwatani, K.; Yamamoto, M.; Terhara, K.; Sesakawa, C.; Suzuki, T.; Nochi, T.; Yokota, Y.; Rennert, P.D.; et al. Intestinal villous Mcells: An antigen entry site in the mucosal epithelium. *Proc. Natl. Acad. Sci. USA* **2004**, *101*, 6110–6115. [CrossRef]
53. Fuglem, B.; Jirillo, E.; Bjerkås, I.; Kiyono, H.; Nochi, T.; Yuki, Y.; Raida, M.; Fischer, U.; Koppang, E.O. Antigen-sampling cells in the salmonid intestinal epithelium. *Dev. Comp. Immunol.* **2010**, *34*, 768–774. [CrossRef]
54. Lovy, J.; Friend, S.E.; Lewis, N.L. Seasonal intestinal coccidiosis in wild bluegill *Lepomis macrochirus* is associated with a spring bacterial epizootic. *J. Fish Dis.* **2019**, *42*, 1697–1711. [CrossRef]
55. Pasnik, D.J.; Smith, S.A.; Lindsay, D.S. Intestinal Coccidiosis in Bluegill, *Lepomis macrochirus*. *J. Parasitol.* **2005**, *91*, 967–970. [CrossRef]
56. Molnár, K.; Hanek, G. Seven new *Eimeria spp.* (Protozoa, Coccidia) from freshwater fishes of Canada. *J. Protozool.* **1974**, *21*, 489–493. [CrossRef] [PubMed]
57. Molnár, K.; Szekely, C.S.; Baska, F. Mass mortality of eel in Lake Balaton due to *Anguillicola crassus* infection. *Bull. Eur. Assoc. Fish Pathol.* **1991**, *11*, 211–212.
58. Silphaduang, U.; Colorni, A.; Noga, E.J. Evidence for widespread distribution of piscidin antimicrobial peptides in teleost fish. *Dis. Aquat. Organ.* **2006**, *72*, 241–252. [CrossRef]
59. Mazon, A.F.; Huising, M.O.; Taverne-Thiele, A.J.; Bastiaans, J.; Verburg-van Kemenade, B.M.L. The first appearance of Rodlet cells in carp (*Cyprinus carpio* L.) ontogeny and their possible roles during stress and parasite infection. *Fish Shellfish Immunol.* **2007**, *22*, 27–37. [CrossRef]
60. Manera, M.; Dezfuli, B.S. Rodlet cells in teleosts: A new insight into their nature and functions. *J. Fish. Biol.* **2004**, *65*, 597–619. [CrossRef]

61. Meuchel, L.W.; Thompson, M.A.; Cassivi, S.D.; Pabelick, C.M.; Prakash, Y.S. Neurotrophins induce nitric oxide generation in human pulmonary artery endothelial cells. *Cardiovasc. Res.* **2011**, *91*, 668–676. [CrossRef]
62. Tocchetti, C.G.; Wang, W.; Froehlich, J.P.; Huke, S.; Aon, M.A.; Wilson, G.M.; Di Benedetto, G.; O'Rourke, B.; Gao, W.D.; Wink, D.A.; et al. Nitroxyl improves cellular heart function by directly enhancing cardiac sarcoplasmic reticulum Ca^{2+} cycling. *Circ. Res.* **2007**, *100*, 96–104. [CrossRef] [PubMed]

Disclaimer/Publisher's Note: The statements, opinions and data contained in all publications are solely those of the individual author(s) and contributor(s) and not of MDPI and/or the editor(s). MDPI and/or the editor(s) disclaim responsibility for any injury to people or property resulting from any ideas, methods, instructions or products referred to in the content.